Pergamon

Tetrahedron Letters 43 (2002) 1607–1611

TETRAHEDRON LETTERS

Highly diastereoselective mercury-mediated synthesis of functionalized 2-azabicyclo[3.3.0]octane derivatives

Emerson P. Peçanha,[a,b] Hugo Verli,[a,b] Carlos R. Rodrigues,[a] Eliezer J. Barreiro[a,b] and Carlos A. M. Fraga[a,b,*]

[a]*Laboratório de Avaliação e Síntese de Substâncias Bioativas,*[†] *Faculdade de Farmácia, Universidade Federal do Rio de Janeiro, PO Box 68006, 21944970, Rio de Janeiro, RJ, Brazil*

[b]*Instituto de Química, Universidade Federal do Rio de Janeiro, Rio de Janeiro, RJ, Brazil*

Received 5 December 2001; accepted 2 January 2002

Abstract—In this paper we described the synthesis of the *cis*-2-azabicyclo[3.3.0]octane derivative (**5b**) employing highly diastereoselective mercury(II)-mediated intramolecular amino-cyclization, followed by reductive demercuration of ethyl *erythro*-1-allyl-2-amino-1-cyclopentanecarboxylate (**7b**). Molecular dynamic studies were performed in order to find a suitable explanation of the diastereoselectivity of azamercuration in comparison with corresponding oxymercuration process.

The *cis*-2-azabicyclo[3.3.0]octane (**1**) heterocycle has proved to be an important structural sub-unit present in several classes of drugs, e.g. the antihypertensive angiotensin converting enzyme inhibitor ramipril[1] (**2**) and the carbamate acetylcholinesterase inhibitor[2] (**3**). Additionally, this bicyclic ring was identified in the backbone of many quinoline[3] and indole[4] alkaloids as well as the framework of many ligands for enantioselective catalysis,[5] e.g. Corey's oxazaborolidine[6] (**4**) (Fig. 1).

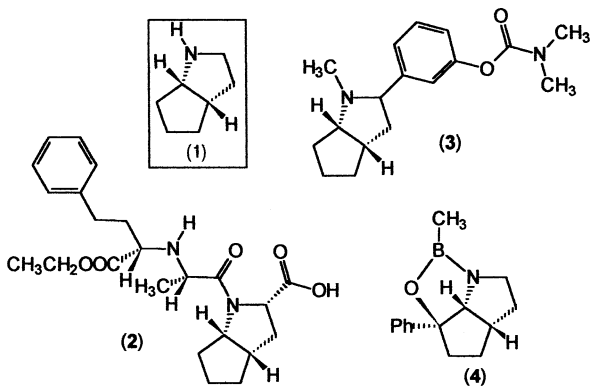

Figure 1. Derivatives presenting *cis*-2-azabicyclo[3.3.0]octane system (**1**).

In previous papers, we described the use of functionalized 2-azabicyclo[3.3.0]octane derivatives (**5a**–**b**) and its oxa-isosteric analogues (**6a**–**b**) as synthons useful in the construction of new bioactive compounds.[7]

In this paper, we report our studies of the cyclization of γ-heterosubstituted olefins mediated by mercury salts as a strategy[8] to achieve stereocontrol in the construction of the C-3 center (Scheme 1). The mercury-mediated heterocyclization is frequently described as a diastereoselective process,[9] and information regarding the mechanism of stereocontrol is widely available.[10]

The cyclization precursors (**7**–**8**) were obtained in two steps, from commercially available methyl 2-oxocyclopentanecarboxylate[11] (**9a**) or ethyl 2-oxocyclopentanecarboxylate[12] (**9b**). The first step consisted of the regioselective *C*-alkylation of the β-ketoesters (**9a**) and (**9b**), employing allyl bromide under Barco's conditions,[13] producing the derivatives (**10a**) and (**10b**), respectively, both in 95% yield (Scheme 2). The reduction of the allyl ketoesters (**10a**) and (**10b**) with sodium borohydride (Table 1, entries 3 and 4) furnished respectively, an *erythro*/*threo* mixture of cyclopentanol derivatives (**8a**) and (**8b**), as described previously.[14] On the other hand, an *erythro*/*threo* mixture of cyclopentylamine derivatives (**7a**) and (**7b**) was obtained by the reductive amination of the compounds (**10a**) and (**10b**), employing ammonium acetate and sodium cyanoborohydride[15] (Table 1, entries 1 and 2).

* Corresponding author. Tel.: +55-21-22609192; fax: +55-21-22733890; e-mail: cmfraga@pharma.ufrj.br

† http://www.farmacia.ufrj.br/lassbio

0040-4039/02/$ - see front matter
PII: S0040-4039(02)00074-6

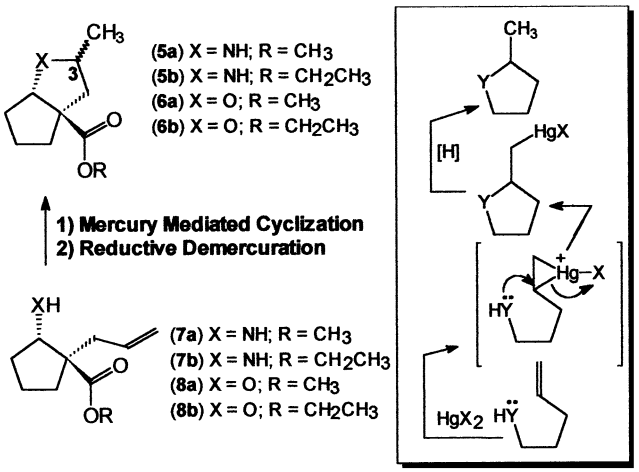

Scheme 1.

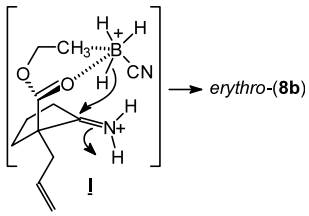

Scheme 2.

The rational for the unexpected diastereomeric excess (75%, Table 1, entry 2) in reductive amination of the ethyl ester (**10b**) could be due the participation of chelated six-membered species **I**, stabilized by additional charge-transfer interaction with terminal methyl group (Scheme 2), which favored the hydride attack to the Si face of the imine group.[16]

The mercury-mediated cyclization[17] of *erythro* derivatives (**7**–**8**) was performed employing mercury acetate (1 equiv.) in CH_2Cl_2 for 10 min at rt, followed by the reductive demercuration of the organomercurial intermediates with $NaBH_4$ (4 equiv.) in 5% aq. NaOH solution for 1 h at room temperature (Table 2). The functionalized *cis*-2-aza- or *cis*-2-oxabicyclo[3.3.0]-octane derivatives (**5a**,**b**) and (**6a**,**b**) were obtained, in yields ranging from 55–71%,[18] as a diastereomeric *endo*/*exo* mixture, which ratio was determined by ^{1}H NMR spectroscopy[19] and confirmed by GC–MS analysis[20] (Table 2). Additionally, after separation by silica gel column chromatography, the relative configuration of the *endo* and *exo* diastereomers of bicyclic compounds (**5**–**6**) was elucidated by NOE experiments (Fig. 2), being in agreement with previous related papers.[7,14,21]

The diastereoselectivity of this cyclization process was largely dependent on the nature of the heteroatom. While the oxymercuration of compounds (**6a**,**b**) presented a very low diastereoselectivity (Table 2, entries 3 and 4), the azamercuration of the derivative (**7b**) furnished the *endo*-isomer of (**5b**) in 90% d.e.[22]

It is believed that the preparation of 2-aza- or 2-oxabicyclic derivatives (**5**–**6**) should take place after the $AcHg^+$ ion coordinates the C=C bond of the allyl group, generating a three member mercuronium ion (Scheme 1). Subsequently, the '5-*exo*-trig' cyclization process[23] occurs through nucleophilic attack of the nitrogen or oxygen atom from the corresponding cyclopentylamines (**7**) or cyclopentanol derivatives (**8**) on the eletrophilic methine carbon of the mercurinane heterocycle.

To elucidate the origins of the diastereoselectivity in the azamercuration process, we submitted the compounds **7**–**8** to theoretical study using semiempirical PM3 method at the SCF-MO level in the gas and solvent phases, with full geometry optimization implemented on a Pentium III 900 MHz computer.[24,25] The different diastereoselectivity profile of oxa- versus azamercuration process was investigated by comparison of the electrostatic potential of the heteroatoms that can assist the anchorage of the $AcHg^+$ to the double bond, i.e. N

Table 1. Reductive preparation of cyclopentylamines (**7a**,**b**) and cyclopentanols (**8a**,**b**) from 2-allyl-2-alkoxycarbonylcyclopentanones (**10a**,**b**)

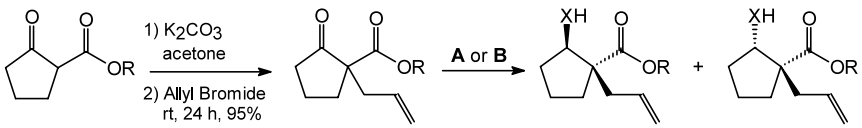

Entry	Compound	X	R	Conditions	Yield (%)	Diastereomeric ratio *threo*:*erythro*[c]
1	**7a**	NH	CH_3	$AcONH_4$, $NaBH_3CN$, MeOH, reflux, 3 h[a]	73	1:4
2	**7b**	NH	CH_2CH_3	$AcONH_4$, $NaBH_3CN$, MeOH, reflux, 3 h[a]	74	1:7
3	**8a**	O	CH_3	$NaBH_4$, MeOH, 0°C, 30 min[b]	97	1:4
4	**8b**	O	CH_2CH_3	$NaBH_4$, MeOH, 0°C, 30 min[b]	98	1:1.8

[a] Condition **A**.
[b] Condition **B**.
[c] Ratios determined by ^{1}H NMR spectra[19] and GC–MS analysis of the crude mixture.[20]

Table 2. Mercury mediated heterocyclization of cyclopentane derivatives (**7**–**8**)

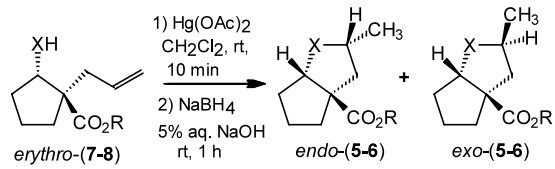

Entry	Compound	X	R	Yield (%)	Diastereomeric ratio *endo*:*exo*[a]
1	**5a**	NH	CH_3	64	3:1
2	**5b**	NH	CH_2CH_3	71	19:1
3	**6a**	O	CH_3	58	1:1.6
4	**6b**	O	CH_2CH_3	55	1:1.1

[a] Ratios determined by ^{1}H NMR spectra[19] and GC–MS analysis of the crude mixture.[20]

versus O (**7a**,**b**) and O versus O (**8a**,**b**) (Fig. 3). The electrostatic potential surface map of the minimal energy conformations of (**7**) and (**8**), obtained after single-point ab initio calculation using 3-21G* basis set[26] with SPARTAN 1.0.5 program,[27] indicated that the absence of diastereoselectivity in the oxymercuration process of derivatives (**7a**,**b**) is due to the similar electrostatic potential occurring near the carbonyl oxygen atom and hydroxyl group, which induces the equal approximation of $AcHg^+$ ion to the *Re* and *Si* faces of the double bond (Fig. 3). On the other hand, in the cyclopentylamine derivatives (**8a**,**b**) the carbonyl oxygen atom of the ester group presented a major electrostatic potential than the amino group at C-2, inducing the stereoselective approximation of the $AcHg^+$ ion to the *Re* face of double bond and driving the diastereoselective formation of the *endo* derivatives (**5a**,**b**) (Fig. 3).

Additionally, molecular modeling studies were performed in order to obtain the energies of transition states (TS) of the cyclization step that culminated in *endo* versus *exo* products (**5**–**6**). The activation energy of the '*endo*-TS' was ten times more stable than '*exo*-TS', independently of the nature of the R group (methyl versus ethyl). These results show that the cyclization step is not directly related to the diastereoselectivity profile described in Table 2. In view of these results, we suggest that coordination of the $AcHg^+$ ion with the double bond could be crucial to the understanding the diastereoselectivity of this reaction. Moreover, the ethyl group may play an important role in this process (entries 1 and 2, Table 2). Accordingly, we calculated the energy barrier associated with the freedom degrees of the ethyl substituent in the ester group of (**7b**). This study was carried out using two theoretical approaches that mimic the effect of the solvent dichloromethane in the conformations of (**7**), i.e. PM3-COSMO[28] and MD.[29] In the first system, the solvent is represented by its permitivity value ($\varepsilon = 8.65$). In the second, one box was constructed and 480 molecules of dichloromethane were strategically placed on it. In both systems, it was found that a large number of conformations has the ethyl group neighborhood in the proximity of the carbonyl group (dihedral angle $\theta = \pm 110°$) (Fig. 4). We suggest that the ethyl group provide an additional stabilization of the $AcHg^+$ ion, favoring its anchorage to the *Re* face of the allylic double bond, explaining the major formation of the *endo* product (**5**).

We conclude that the larger electrostatic potential of the carbonyl group of the compound (**7b**) associated with the rotation of its ethyl group, are factors that contribute to the stabilization of the complexation of the $AcHg^+$ ion on the *Re* face of the double bond, leading to the diastereoselective formation of the *endo* product (**5b**).

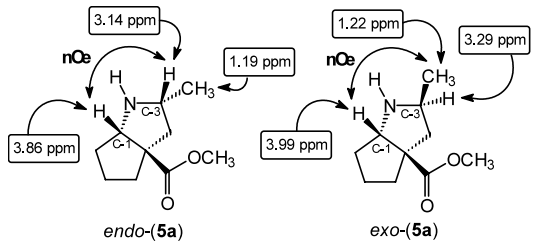

Figure 2. Elucidation of the relative configuration of *endo*/*exo* isomers of the bicyclic derivatives (**5a**,**b**) and (**6a**,**b**) using NOE experiments.

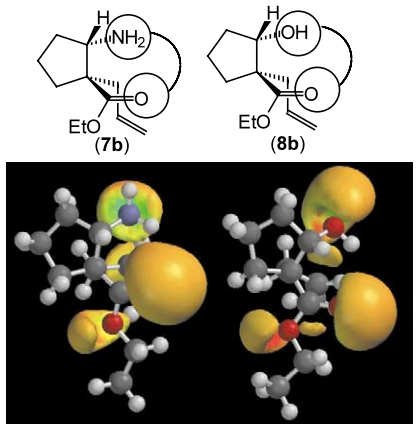

Figure 3. 3D isoenergy contours of MEP for compounds (**7b**) and (**8b**). Solid contours have −20 kcal/mol electrostatic interaction energy.

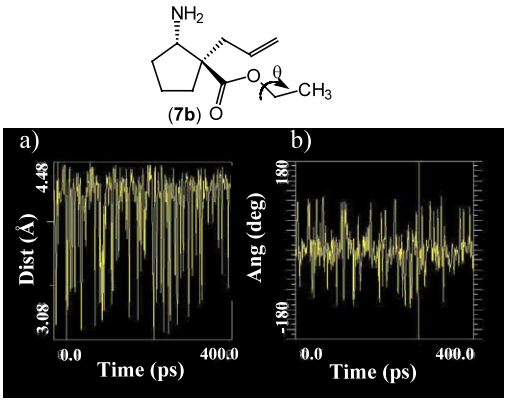

Figure 4. Simulation of time dependent solvation of the compound (**7b**): (a) distance between terminal methyl group and carbonyl oxygen; (b) dihedral angle (θ) analyses.

Acknowledgements

Thanks are due to CNPq (BR., grants #50.0033/96-5, #460200/00-3 and fellowships), FAPERJ (BR.) and FUJB (BR.) for financial support. We are grateful to Analytical Center of NPPN (UFRJ-BR.) for spectroscopic facilities. We are indebted to Professor Carlos M. R. Sant'Anna (UFRRJ–BR.) for molecular modeling suggestions.

References

1. Ling, R.; Yoshida, M.; Mariano, P. S. *J. Org. Chem.* **1996**, *61*, 4439–4449.
2. Borioni, A.; Del Giudice, M. R.; Mustazza, C.; Gatta, F. *J. Heterocyclic Chem.* **2000**, *37*, 799–810.
3. (a) Schultz, A.; Dai, M. *Tetrahedron Lett.* **1999**, *40*, 645–648; (b) Palmisano, G.; Danieli, B.; Lesma, G.; Mauro, M. *J. Chem. Soc., Chem. Commun.* **1986**, *113I*, 1564–1565.
4. Hugel, G.; Cossy, J.; Levy, J. *Tetrahedron Lett.* **1987**, *28*, 1773–1776.
5. (a) Wallbaum, S.; Martens, J. *Tetrahedron: Asymmetry* **1993**, *4*, 637–640; (b) Wilken, J.; Gröger, H.; Kossenjans, M.; Martens, J. *Tetrahedron: Asymmetry* **1997**, *16*, 2761–2771; (c) Aurich, H. G.; Soeberdt, M. *Tetrahedron Lett.* **1998**, *39*, 2553–2554.
6. Corey, E. J.; Chen, C.-P.; Reichard, G. A. *Tetrahedron Lett.* **1989**, *30*, 5547–5550.
7. (a) Fraga, C. A. M.; Miranda, A. L. P.; Barreiro, E. J. *Chem. Pharm. Bull.* **1996**, *44*, 2157–2161; (b) Peçanha, E. P.; Fraga, C. A. M.; Barreiro, E. J. *Farmaco* **1998**, *53*, 327–336; (c) Barreiro, E. J.; Fraga, C. A. M.; Peçanha, E. P. *Trends Heterocyclic Chem.* **1999**, *6*, 37–48; (d) Santos, M. R. L.; Barreiro, E. J.; Braz-Filho, R. *Tetrahedron* **2000**, *56*, 5289–5295; (e) Peçanha, E. P.; Fraga, C. A. M.; Barreiro, E. J.; Braga, M. F. M.; Pereira, E. F. R.; Albuquerque, E. X. *J. Braz. Chem. Soc.* **2001**, *12*, 408–412.
8. Nordvall, G.; Sundquist, S.; Glas, G.; Gogoll, A.; Nilverbrant, L.; Hacksell, U. *J. Med. Chem.* **1992**, *35*, 1541–1550.
9. (a) Tius, M. A.; Bush-Petersen, J. *Tetrahedron Lett.* **1994**, *56*, 4289–5295; (b) Imagawa, H.; Shigaraki, T.; Suzuki, T.; Takao, H.; Yamada, H.; Sugihara, T.; Nishizawa, M. *Chem. Pharm. Bull.* **1998**, *46*, 1341–1342.
10. Garavelas, A.; Mavropoulos, I.; Perlmutter, P.; Westman, G. *Tetrahedron Lett.* **1995**, *36*, 463–466.
11. Purchased from Aldrich Co., Milwaukee, USA.
12. Derivative synthesized in 71% yield from Dieckmann cyclization of ethyl adipate, using $AlCl_3/Et_3N$ in CH_2Cl_2. For a detailed description, see: Peçanha, E. P.; Barreiro, E. J.; Fraga, C. A. M. *Quimica Nova* **1997**, *20*, 435–437.
13. Barco, A.; Benetti, S.; Pollini, G. P. *Synthesis* **1973**, 316.
14. (a) Fraga, C. A. M.; Barreiro, E. J. *Synth. Commun.* **1995**, *25*, 1133–1144; (b) Teixeira, L. H. P.; Barreiro, E. J.; Fraga, C. A. M. *Synth. Commun.* **1997**, *27*, 3241–3257.
15. Banwell, M. G.; Bui, C. T.; Pham, H. T. T.; Simpson, G. W. *J. Chem. Soc., Perkin Trans. 1* **1996**, 967–969.
16. Menezes, C. M. S.; Teixeira, L. H. P.; Sant' Anna, C. M. R.; Rodrigues, C. R.; Barreiro, E. J.; Fraga, C. A. M. **2001**, unpublished results. These data were obtained from molecular modeling studies, using semiempirical PM3 method.
17. Roubaud, V.; Le Moigne, F.; Mercier, A.; Tordo, P. *Synth. Commun.* **1996**, *26*, 1507–1516.
18. The 2-azabicyclo[3.3.0]octane derivatives (**5a**) and (**5b**) were obtained as a mixture of free secondary amines and $NH–BH_3$ complexes. This mixture were converted into desired free secondary amines after acidic treatment.
19. ^1H and ^{13}C NMR spectra were determined in $CDCl_3$/TMS, with UNITY plus-300 at 300 and 75 MHz, respectively.
20. GC–MS was performed in a HP-5972A Gas-chromatography-mass-spectrometer provided with a HP-5ms capillary column (30 m×250 μm×0.25 μm, 70–290°C, at 10°C/min).
21. Peçanha, E. P.; Fraga, C. A. M.; Barreiro, E. J. *Heterocycles* **1998**, *48*, 2621–2630.
22. None bicyclic derivative presenting *trans* ring junction was found.
23. Baldwin, J. E. *J. Chem. Soc., Chem. Commun.* **1976**, *1*, 734–736.
24. (a) Stewart, J. J. P. *J. Comp. Chem.* **1989**, *10*, 209; (b) Stewart, J. J. P. *J. Comp. Chem.* **1991**, *12*, 320–341; (c) MOPAC 93.00, Stewart, J. J. P., Fujitsu Limited, Tokyo, Japan, 1993.
25. The PM3 method shows a better simulation of ^+HgAc ion than AM1 method, e.g. keeping the coordination between the mercury atom and the two oxygen atoms.
26. Hessian matrix analyses were employed to unequivocally characterize them as true minima potential energy surface.
27. Wavefunction Inc., Irvine, CA, 2000.
28. The COSMO (conductor-like screening model) solvation model was used to construct a solvent accessible surface area based on van der Waals radius. The relative permitivity of CH_2Cl_2 was taken to be $\varepsilon=8.65$ and the model incorporated up to 30 surfaces segments per atom, then we set the parameter NPPA to 1082 and NSPA to 42. The effective VDW radius of the solvent molecule was 2.69 Å. All structures were optimized to a gradient norm <0.1 in the gas phase and <0.6 in the solvent phase, using the eigenvector method (EF) at PRECISE level. Parallel to these methods a molecular dynamics simulation of (**7**)

was performed in a previously validated solution of CH_2Cl_2.

29. Initially the system was minimized for 10,000 steps of a steepest descent algorithm followed by 10,000 steps of a conjugated gradient algorithm (derivatives less than 0.01 kcal mol^{-1} $Å^{-1}$). The packed system was placed in a cubic box of 40 $Å^3$. The properties of the pure liquid were calculated via molecular dynamics (MD) simulations with periodic boundary conditions, using no constraints, and a time step of 1 fs. The *NPT* ensemble corresponding to the usual experimental conditions was applied. A residue-based cutoff of 20 Å was applied. A 400 ps MD simulation was performed using the last 300 ps to collect data. Experimental density of liquid CH_2Cl_2 was used to validate the theoretical model ($\rho^{303,15} = 1{,}3078$). The all-atom CVFF forcefield within the Discover program (version 2.9.7) was employed in all the performed calculations.